



*Citation for published version:*

Shardlow, T & Mills, A 2008, 'Analysis of the geodesic interpolating spline', *European Journal of Applied Mathematics*, vol. 19, no. 5, pp. 519-539. <https://doi.org/10.1017/S0956792508007493>

*DOI:*

[10.1017/S0956792508007493](https://doi.org/10.1017/S0956792508007493)

*Publication date:*

2008

*Document Version*

Publisher's PDF, also known as Version of record

[Link to publication](#)

© 2008 Cambridge University

## University of Bath

### General rights

Copyright and moral rights for the publications made accessible in the public portal are retained by the authors and/or other copyright owners and it is a condition of accessing publications that users recognise and abide by the legal requirements associated with these rights.

### Take down policy

If you believe that this document breaches copyright please contact us providing details, and we will remove access to the work immediately and investigate your claim.

# Analysis of the Geodesic Interpolating Spline

Anna Mills and Tony Shardlow

*School of Mathematics, The University of Manchester, Manchester M60 1QD, UK*

*(Received 31 October 2012)*

We study the Geodesic Interpolating Spline with a biharmonic regulariser for solving the landmark image registration problem. We show existence of solutions, discuss uniqueness, and show how the problem can be efficiently solved numerically. The main advantage of the Geodesic Interpolating Spline is that it provides a diffeomorphism and we show this is preserved under our numerical approximation.

## 1 Introduction

Image registration is the process of aligning desired features in two or more images, to which there are several approaches, as described in [17]. Landmark-based pairwise registration considers registering two images, each with a set of landmarks marked, with a correspondence defined between the two sets of landmarks, where one of the images is to be registered to the other by a nonlinear warp so that the landmarks on the template image,  $T$ , are exactly aligned with with the corresponding landmarks on the reference image,  $R$ . We study the technique for solving this problem known as the Geodesic Interpolating Spline (GIS). We consider a family of warps  $\Phi: \Omega \rightarrow \Omega$ , where  $\Omega$  is the domain of the image, defined by the initial value problem

$$\Phi(\mathbf{P}) = \mathbf{x}(1) \quad \text{where} \quad \frac{d\mathbf{x}}{dt} = \mathbf{v}(\mathbf{x}, t), \quad \mathbf{x}(0) = \mathbf{P}, \quad (1.1)$$

and  $\mathbf{v}: \Omega \times [0, 1] \rightarrow \mathbb{R}^d$  is a time dependent deformation field. The GIS landmark problem is to choose a warp  $\Phi$  that satisfies the landmark matching conditions and minimises the energy in the field  $\mathbf{v}$ . In particular, we seek to minimise the energy

$$l(\mathbf{x}_i(t), \mathbf{v}(t, \mathbf{x})) = \int_0^1 \int_{\Omega} \|L\mathbf{v}(t, \mathbf{x})\|^2 d\mathbf{x} dt, \quad (1.2)$$

over deformation fields,  $\mathbf{v}(t, \mathbf{x}) \in \mathbb{R}^d$  and paths,  $\mathbf{x}_i(t) \in \Omega$  for  $i = 1, \dots, n_c$ , where  $L$  is a constant-coefficient, differential operator, and such that

$$\frac{d\mathbf{x}_i}{dt} = \mathbf{v}(t, \mathbf{x}_i(t)), \quad 0 \leq t \leq 1, \quad (1.3 a)$$

and

$$\mathbf{x}_i(0) = \mathbf{P}_i, \quad \text{and} \quad \mathbf{x}_i(1) = \mathbf{Q}_i, \quad i = 1, \dots, n_c, \quad (1.3 b)$$

where  $\mathbf{P}_i$  and  $\mathbf{Q}_i$  for  $i = 1, \dots, n_c$  are knot points on, respectively, the template image,  $T$ , and the reference image,  $R$ . In this paper, we focus on the energy,  $l$ , defined by

the Laplacian,  $L = \Delta$  in (1.2), which models the Willmore energy or bending energy arising in the deformation of thin plates, as described in [6]. In information theory, the energy  $l$  can also be interpreted as the minimum description or code length required to send the warp parameters, when we assume the parameters are modelled by the Gibbs distribution. This viewpoint is outlined further in [15].

The GIS technique has been developed by [4, 7, 10, 8, 22] and is intended to overcome the difficulties of thin plate splines [3] that lead to folding or tearing of the image in the case of large deformations. The use of velocity fields and an optical flow allows us to deform the image in a sequence of small steps and the mapping,  $\Phi$  is known to be a diffeomorphism. This is important as we do not wish to lose any information from the image, and for some implementations we require the mapping to be invertible. Problems involved in using non-invertible mappings are discussed in [9]. The necessity for mappings to be diffeomorphic is discussed in [10]. A similar method is defined for vector fields discretised on grids in [11].

The paper is organised as follows. In section 2, we study existence of a minimising deformation field  $\mathbf{v}$  and distinguished paths  $\mathbf{x}_i$  (corresponding to each landmark). We base our analysis on the work of Dupuis [7] and extend their result to include the biharmonic energy. In [7], it is assumed that functions in the domain of  $L$  have Lipschitz regularity, which excludes the biharmonic case ( $L = \Delta$ ). Further, we develop the analysis for landmark matching, rather than applying the penalty term used in [7]. In section 3, we show how the deformation field can be expressed as a linear combination of Green's functions and hence show that the deformation field is unique given a set of paths  $\mathbf{x}_i$ . In this situation, we choose  $\Omega$  to be the unit ball in  $\mathbb{R}^2$  and apply homogeneous Dirichlet and Neumann conditions, so we have use of an explicit biharmonic Green's function. These boundary conditions are satisfied by the Biharmonic Green's function derived by Boggio [2]:

$$G(\mathbf{x}, \mathbf{y}) = |\mathbf{x} - \mathbf{y}|^2 \left( \frac{1}{2}(A^2 - 1) - \ln A \right), \quad (1.4 a)$$

where

$$A(\mathbf{x}, \mathbf{y}) = \frac{\sqrt{|\mathbf{x}|^2 |\mathbf{y}|^2 - 2\mathbf{x} \cdot \mathbf{y} + 1}}{|\mathbf{x} - \mathbf{y}|}, \quad (1.4 b)$$

where  $\mathbf{x}$  and  $\mathbf{y}$  are two-dimensional vectors. In section 4, we show how to rewrite the optimisation problem (1.2) as a shooting problem for a Hamiltonian system and discuss its efficient numerical solution. In section 5, we show that the diffeomorphism property of the warp is preserved under numerical approximation for the case  $d = 2$ . Finally, in section 6, we show that in general there is no unique global minimum to the GIS landmark problem.

## 2 Existence

We investigate the existence of minimizing paths and deformation fields for the Geodesic Interpolating Spline problem (1.2). Based on the work of Dupuis, Grenander and Miller [7], we show the existence of minimizing paths and vector fields.

First we define the spaces that give the setting of the problem. We work in the space

$V = L_2([0, 1] : H \times \dots \times H)$ , where we have the  $d$ -times product, where  $d$  is typically 2 or 3, of the space

$$H = \{h \in H^2(\Omega) : h = 0 \text{ and } \frac{\partial h}{\partial \mathbf{n}} = 0 \text{ on } \partial\Omega\},$$

for the domain  $\Omega \subset \mathbb{R}^d$ , where  $\Omega$  is smooth and bounded. The vector  $\mathbf{n}$  is the unit normal on  $\partial\Omega$  the boundary of the domain,  $\Omega$ , and

$$H^2(\Omega) = \{\text{all distributions } h : \Omega \rightarrow \mathbb{R} \text{ such that } D^\alpha h \in L_2(\Omega), |\alpha| \leq 2\},$$

where  $D^\alpha u$  represents all derivatives of total order  $\leq \alpha$  and

$$L_2(\Omega) = \left\{ f : \Omega \rightarrow \mathbb{R} \text{ such that } \left( \int_{\Omega} |f(x)|^2 dx \right)^{\frac{1}{2}} < \infty \right\}.$$

Define the norms

$$\|\mathbf{v}\|_V^2 = \sum_{k=1}^d \int_0^1 \|v_k(\cdot, t)\|_H^2 dt, \quad \text{for } \mathbf{v} = (v_1, \dots, v_d) \in V, \quad v_k(\cdot, t) \in H,$$

where

$$\|h\|_H^2 = \int_{\Omega} \|\Delta h\|_{\mathbb{R}^d}^2 dx, \quad h \in H.$$

The space  $C^1([s, t] : \Omega)$  is the set of continuous functions from  $[s, t]$  to  $\Omega$  with continuous first derivatives with norm defined by

$$\|f\|_{C^1([s, t] : \Omega)} = \sum_{j=0}^1 \left\| \frac{\partial^j f}{\partial t^j} \right\|_{C([s, t] : \Omega)}$$

where

$$\|f\|_{C([s, t] : \Omega)} = \sup_{s \leq r \leq t} \|f(r)\|_{\mathbb{R}^d}.$$

The space  $C^1(\Omega : \mathbb{R})$ , abbreviated to  $C^1(\Omega)$ , is the space of continuous functions from  $\Omega$  to  $\mathbb{R}$  with continuous first derivatives. The corresponding norm is given by

$$\|f\|_{C^1(\Omega)} = \|f\|_{C(\Omega : \mathbb{R})} + \sum_{i=1}^d \left\| \frac{\partial f}{\partial x_i} \right\|_{C(\Omega : \mathbb{R})}$$

where

$$\|f\|_{C(\Omega : \mathbb{R})} = \sup_{\mathbf{x} \in \Omega} \|f(\mathbf{x})\|_{\mathbb{R}}.$$

**Proposition 1** *Let  $0 < \alpha < \frac{1}{2}$ . Then there exists  $C < \infty$  such that for all  $\mathbf{f} \in H \times \dots \times H$  and for all  $\mathbf{x}, \mathbf{y} \in \Omega$ ,  $d = 2, 3$*

$$\|\mathbf{f}(\mathbf{x}) - \mathbf{f}(\mathbf{y})\|_{\mathbb{R}^d} \leq C \|\mathbf{f}\|_{H \times \dots \times H} |\mathbf{x} - \mathbf{y}|^\alpha. \quad (2.1)$$

**Proof** Working with the components,  $f_k \in H, k = 1, \dots, d$  of  $\mathbf{f}$ , the Compact Embedding Lemma states that there exists  $C < \infty$  such that

$$|f_k(\mathbf{x}) - f_k(\mathbf{y})| \leq C \|f_k\|_H |\mathbf{x} - \mathbf{y}|^\alpha,$$

where  $0 < \alpha < 1$  for  $d = 2$  and  $0 < \alpha < 1/2$  for  $d = 3$ . By definition of the  $\mathbb{R}^d$  norm,

$$\begin{aligned} \|\mathbf{f}(\mathbf{x}) - \mathbf{f}(\mathbf{y})\|_{\mathbb{R}^d} &= \left( \sum_{k=1}^d (f_k(\mathbf{x}) - f_k(\mathbf{y}))^2 \right)^{\frac{1}{2}} \\ &\leq \left( \sum_{k=1}^d (C \|f_k\|_H |\mathbf{x} - \mathbf{y}|^\alpha)^2 \right)^{\frac{1}{2}} \\ &\leq C |\mathbf{x} - \mathbf{y}|^\alpha \left( \sum_{k=1}^d \|f_k\|_H^2 \right)^{\frac{1}{2}} \\ &\leq C \|\mathbf{f}\|_{H \times \dots \times H} |\mathbf{x} - \mathbf{y}|^\alpha. \end{aligned}$$

□

This gives us Hölder continuity for  $\mathbf{f} \in H \times \dots \times H$ .

We show that minimizing paths and corresponding vector fields exist for (1.2). We examine (control point) paths  $\mathbf{x}_i \in C^1([0, 1] : \Omega)$ ,  $i = 1, \dots, n_c$  and deformation fields  $\mathbf{v} \in V$ ,  $\mathbf{v} = (v_1, \dots, v_d)$ , on  $\mathbf{x} \in \Omega$ , where  $n_c$  is the number of control points used.

**Theorem 1** *We assume that there exists at least one deformation field,  $\mathbf{v} \in V$ , and control point paths,  $\mathbf{x}_i \in C^1([0, 1] : \Omega)$ , such that*

$$\mathbf{x}_i(0) = \mathbf{P}_i, \quad \mathbf{x}_i(1) = \mathbf{Q}_i, \quad i = 1, \dots, n_c, \quad (2.2)$$

where  $\mathbf{P}_i$  and  $\mathbf{Q}_i$  give, respectively, the initial and final control point positions in  $\Omega$ , and  $\mathbf{x}_i(t) \in \Omega$  represents the control point path  $\mathbf{x}_i$  at time  $t$ , conforming to the constraint

$$\frac{d\mathbf{x}_i(t)}{dt} = \mathbf{v}(\mathbf{x}_i(t), t). \quad (2.3)$$

We describe such deformation fields and control paths as being in the feasible set

$$\mathcal{F} = \left\{ (\mathbf{v}, \{\mathbf{x}_i, i = 1, \dots, n_c\}) \in V \times C^1([0, 1] : \Omega)^{n_c} : (2.2) \text{ and } (2.3) \text{ hold} \right\}.$$

Then there exist deformation fields and control point paths in the feasible set that minimise  $\|\mathbf{v}\|_V^2$ .

**Proof** By assumption, the feasible set is non-empty.

We begin by examining a sequence of deformation fields and paths,  $(\mathbf{v}^n, \{\mathbf{x}_i^n, i = 1, \dots, n_c\}) \in \mathcal{F}$  such that  $\|\mathbf{v}^n\|_V \rightarrow \inf \|\mathbf{v}\|_V$  where the limit is over deformation fields and paths. Without loss of generality, in order to use the Banach-Alaoglu Theorem (see [20] for a statement of the theorem) to show convergence of a subsequence, we assume that the sequence is bounded above, so that we have

$$\|\mathbf{v}^n\|_V \leq M, \quad (2.4)$$

for some  $M < \infty$ .

By the Banach-Alaoglu Theorem we know that  $\mathbf{v}^n$ , a sequence of deformation fields in the feasible set, has a weakly convergent subsequence,  $\mathbf{v}^{n_m} \in V$ , so that we can write  $\mathbf{v}^{n_m} \rightharpoonup \mathbf{v}^*$  for some weak limit  $\mathbf{v}^* \in V$ .

By weak lower semi-continuity of the norm, we have

$$\|\mathbf{v}^*\|_V^2 \leq \liminf_{m \rightarrow \infty} \|\mathbf{v}^{n_m}\|_V^2. \quad (2.5)$$

We assume that there are paths  $\mathbf{x}_i^*, i = 1, \dots, n_c$  such that we have  $(\mathbf{v}^*, \{\mathbf{x}_i^*, i = 1, \dots, n_c\}) \in \mathcal{F}$  which will be shown later in the proof. With this assumption we see that

$$\|\mathbf{v}^*\|_V^2 \geq \liminf_{n \rightarrow \infty} \|\mathbf{v}^n\|_V^2, \quad (2.6)$$

since  $\mathbf{v}^*$  with associated paths is always in the feasible set, so its norm must be greater than or equal to the infimum limit of the norm of the elements of the feasible set. Therefore, from (2.5) and (2.6), we have

$$\liminf_{n \rightarrow \infty} \|\mathbf{v}^n\|_V^2 = \liminf_{m \rightarrow \infty} \|\mathbf{v}^{n_m}\|_V^2 = \|\mathbf{v}^*\|_V^2, \quad (2.7)$$

so the sequence of deformation fields tends to the minimum.

We now examine the paths for the mappings. We want to show that we have a sequence of paths,  $\mathbf{x}^n(s; t, \mathbf{x})$  such that

$$\begin{aligned} \frac{d}{ds} \mathbf{x}^n(s; 1, \mathbf{x}) &= \mathbf{v}^n(\mathbf{x}^n(s; 1, \mathbf{x}), s) \\ \mathbf{x}^n(1; 1, \mathbf{x}) &= \mathbf{x}. \end{aligned} \quad (2.8)$$

We show that this sequence behaves such that  $\mathbf{x}^n \rightarrow \mathbf{x}^*$  on  $C^1([0, 1] : \Omega)$ , where  $\mathbf{x}^*$  solves the ordinary differential equations

$$\begin{aligned} \frac{d}{ds} \mathbf{x}^*(s; 1, \mathbf{x}) &= \mathbf{v}^*(\mathbf{x}^*(s; 1, \mathbf{x}), s) \\ \mathbf{x}^*(1; 1, \mathbf{x}) &= \mathbf{x}, \end{aligned} \quad (2.9)$$

the derivatives being taken with respect to  $s$ .

Before proceeding with the proof, we obtain an important result about the solution of (2.9). Because  $\mathbf{v} \in V$ , the deformation field  $\mathbf{v}$  is continuous and by standard ODE theory a solution to (2.9) exists. Hence, the system (2.9) gives us a flow across the whole domain. We only set constraints (2.2), (2.3) on the control point paths, but results that hold for the whole domain will apply to control point paths.

We take a control point,  $\mathbf{x} \in \Omega$ . In order to apply the Arzela-Ascoli theorem to our sequence of paths to show the existence of a convergent subsequence, we want to show  $\{\mathbf{x}^n(\cdot; 1, \mathbf{x})\}$  to be compact in  $C([t - \delta, t + \delta] : \mathbb{R}^d)$  for small  $\delta$ . We have

$$\|\mathbf{x}^n(t; 1, \mathbf{x}) - \mathbf{x}^n(s; 1, \mathbf{x})\|_{\mathbb{R}^d} = \left\| \int_s^t \mathbf{v}^n(\mathbf{x}^n(r; t, \mathbf{x}), r) dr \right\|_{\mathbb{R}^d} \quad (2.10)$$

$$\leq \int_s^t \|\mathbf{v}^n(\mathbf{x}^n(r; t, \mathbf{x}), r)\|_{\mathbb{R}^d} dr \quad (2.11)$$

$$\leq \int_s^t \|\mathbf{v}^n(\cdot, r)\|_{C(\Omega; \mathbb{R}^d)} dr. \quad (2.12)$$

Since  $H$  is continuously embedded in  $C(\Omega : \mathbb{R})$  by the Sobolev Embedding Theorem we have, for some  $A < \infty$ ,

$$\|\mathbf{v}^n(\cdot, r)\|_{C(\Omega; \mathbb{R}^d)} \leq A \|\mathbf{v}^n(\cdot, r)\|_{H \times \dots \times H}. \quad (2.13)$$

Hence, we can write

$$\begin{aligned}\|\mathbf{x}^n(t; 1, x) - \mathbf{x}^n(s; 1, x)\|_{\mathbb{R}^d} &\leq A \int_s^t \|\mathbf{v}^n(\cdot, r)\|_{H \times \dots \times H} dr \\ &\leq A \int_0^1 1_{(s,t)}(r) \|\mathbf{v}^n(\cdot, r)\|_{H \times \dots \times H} dr,\end{aligned}$$

where

$$1_{(s,t)}(r) = \begin{cases} 1 & \text{if } r \in (\min(s, t), \max(s, t)) \\ 0 & \text{otherwise} \end{cases}.$$

Applying the Cauchy-Schwarz inequality and evaluating the first integral gives

$$\|\mathbf{x}^n(t; 1, x) - \mathbf{x}^n(s; 1, x)\|_{\mathbb{R}^d} \leq A(t-s)^{\frac{1}{2}} \left( \int_0^1 \|\mathbf{v}^n(\cdot, r)\|_{H \times \dots \times H}^2 dr \right)^{\frac{1}{2}}. \quad (2.14)$$

Using (2.4), we conclude

$$\|\mathbf{x}^n(t; 1, x) - \mathbf{x}^n(s; 1, x)\|_{\mathbb{R}^d} \leq A(t-s)^{\frac{1}{2}} M.$$

This gives us Hölder continuity which gives us equicontinuity for the paths. In order to apply the Arzela-Ascoli Theorem, we also require our sequence to be bounded in the space  $C([t-\delta, t+\delta] : \mathbb{R}^d)$ . We now move to considering control point paths at time  $t$ , so we use the notation  $\mathbf{x}_i^n(t)$ ,  $i = 1, \dots, n_c$  to denote the  $i$ -th control point path at time  $t$ . We have

$$\mathbf{x}_i^n(t) = \mathbf{P}_i + \int_0^t \mathbf{v}^n(\mathbf{x}_i^n(s), s) ds.$$

So we can write

$$\|\mathbf{x}_i^n(t)\|_{\mathbb{R}^d} \leq \|\mathbf{P}_i\|_{\mathbb{R}^d} + \left\| \int_0^t \mathbf{v}^n(\mathbf{x}_i^n(s), s) ds \right\|_{\mathbb{R}^d} \quad (\text{by the triangle inequality}).$$

Examining the last term, we have

$$\begin{aligned}\left\| \int_0^t \mathbf{v}^n(\mathbf{x}_i^n(s), s) ds \right\|_{\mathbb{R}^d} &\leq \int_0^t \|\mathbf{v}^n(\cdot, s)\|_{C(\Omega; \mathbb{R})} ds \\ &\leq A \int_0^t \|\mathbf{v}^n(\cdot, s)\|_{H \times \dots \times H} ds \\ &\leq A \|\mathbf{v}^n\|_V.\end{aligned}$$

Since we assume that the sequence  $\mathbf{v}^n$  is bounded above (2.4) in the norm  $\|\cdot\|_V$ , we see that the sequence  $\mathbf{x}^n$  is bounded above in the norm  $\|\cdot\|_{\mathbb{R}^d}$ . Recalling that our domain is compact, we are able to apply the Arzela-Ascoli theorem, so that we can write a convergent subsequence of  $\mathbf{x}^n$  as  $\phi^n$  with limit  $\phi^*$ .

Adding and subtracting terms, we can write

$$\begin{aligned}\int_t^1 (\mathbf{v}^n(\phi^n(s), s) - \mathbf{v}^*(\phi^*(s), s)) ds &= \int_t^1 (\mathbf{v}^n(\phi^n(s), s) - \mathbf{v}^n(\phi^*(s), s)) ds \\ &\quad + \int_t^1 (\mathbf{v}^n(\phi^*(s), s) - \mathbf{v}^*(\phi^*(s), s)) ds.\end{aligned} \quad (2.15)$$

By Proposition 1, we can estimate the first term of (2.15) as follows, applying the Cauchy-Schwarz inequality as in (2.14)

$$\begin{aligned}
 & \int_t^1 (\mathbf{v}^n(\phi^n(s), s) - \mathbf{v}^n(\phi^*(s), s)) ds & (2.16) \\
 & \leq (1-t)^{\frac{1}{2}} \left( \int_0^1 C \|\mathbf{f}\|_{H \times \dots \times H} \|\phi^n(s) - \phi^*(s)\|_{\mathbb{R}^d}^2 \alpha ds \right)^{\frac{1}{2}} \\
 & \leq C \|\phi^n(s) - \phi^*(s)\|_{C([0,1]:\mathbb{R}^d)}^\alpha \\
 & \rightarrow 0 \text{ since } \phi^n \text{ is a convergent subsequence with limit } \phi^*.
 \end{aligned}$$

To examine the second term, we use the weak convergence of  $\mathbf{v}^n$  to  $\mathbf{v}^*$  in  $C([0,1]:\Omega)$ . We can write  $\mathbf{w}^n = \mathbf{v}^n - \mathbf{v}^* \rightarrow 0$  and define the function  $\mathbf{z}^n \in C(\Omega \times [0,1]:\mathbb{R}^d)$  as

$$\mathbf{z}^n(\cdot, t) = \int_t^1 \mathbf{w}^n(\cdot, s) ds. \quad (2.17)$$

In order to apply the Arzela-Ascoli theorem, we show  $\mathbf{z}^n$  to be bounded and equicontinuous on  $C(\Omega \times [0,1]:\mathbb{R}^d)$ . With  $0 \leq s \leq t \leq 1$  and  $\mathbf{x}, \mathbf{y} \in \Omega$ , we have

$$\begin{aligned}
 \|\mathbf{z}^n(\mathbf{x}, t) - \mathbf{z}^n(\mathbf{y}, s)\|_{\mathbb{R}^d} & \leq \left\| \int_t^1 (\mathbf{w}^n(\mathbf{x}, r) - \mathbf{w}^n(\mathbf{y}, r)) dr \right\|_{\mathbb{R}^d} \\
 & \quad + \left\| \int_s^t \mathbf{w}^n(\mathbf{y}, r) dr \right\|_{\mathbb{R}^d} & (2.18)
 \end{aligned}$$

$$\leq C \|\mathbf{x} - \mathbf{y}\|_{\mathbb{R}^d}^\alpha + (t-s)^{\frac{1}{2}} \|\mathbf{w}^n\|_V, \quad (2.19)$$

using Proposition 1. By the construction of  $\mathbf{v}^n$ ,  $\|\mathbf{w}^n\|_V$  is bounded, and the sequence  $\mathbf{z}^n$  is equicontinuous.

We have

$$\begin{aligned}
 \|\mathbf{z}^n(\mathbf{x}, t)\|_{\mathbb{R}^d} & \leq \|\mathbf{z}^n(\mathbf{x}, 1)\|_{\mathbb{R}^d} + \|\mathbf{z}^n(\mathbf{x}, 1) - \mathbf{z}^n(\mathbf{x}, t)\|_{\mathbb{R}^d} \\
 & \leq A(1-t)^{\frac{1}{2}} \|\mathbf{w}^n\|_V
 \end{aligned}$$

as  $\mathbf{z}^n(\mathbf{x}, 1) = 0$ . So the sequence is bounded.

Hence, by the Arzela-Ascoli theorem, we have  $\mathbf{z}^n \rightarrow \mathbf{z}^*$  for some limit point  $\mathbf{z}^* \in C(\Omega \times [0,1]:\mathbb{R}^d)$ . Since  $\mathbf{w}^n \rightarrow 0$  in  $V$ , we have

$$\int_\Omega \int_0^1 \left\langle \gamma(\mathbf{x}, s), \mathbf{w}^n(\mathbf{x}, s) \right\rangle_{\mathbb{R}^d} ds d\mathbf{x} \rightarrow 0 \quad \forall \gamma \in V.$$

In particular, if  $\gamma(\mathbf{x}, s) = \gamma(\mathbf{x}) 1_{\{s \geq t\}}$ , where

$$1_{\{s \geq t\}} = \begin{cases} 1 & \text{if } s \geq t \\ 0 & \text{otherwise} \end{cases},$$

then we have

$$\int_\Omega \left\langle \gamma(\mathbf{x}), \int_t^1 \mathbf{w}^n(\mathbf{x}, s) ds \right\rangle_{\mathbb{R}^d} d\mathbf{x} \rightarrow 0.$$

Using

$$\mathbf{z}^n(\mathbf{x}, t) = \int_t^1 \mathbf{w}^n(\mathbf{x}, s) ds,$$



we obtain

$$\int_{\Omega} \left\langle \gamma(\mathbf{x}), \mathbf{z}^n(\mathbf{x}, t) \right\rangle_{\mathbb{R}^d} d\mathbf{x} \rightarrow 0.$$

Since this holds for all  $\gamma \in C(\Omega : \mathbb{R}^d)$ , we know  $\mathbf{z}^* = 0$ . So we have shown

$$\int_t^1 (\mathbf{v}^n(\mathbf{x}, s) - \mathbf{v}^*(\mathbf{x}, s)) ds \rightarrow 0 \quad \text{as } n \rightarrow \infty, \forall \mathbf{x} \in \Omega. \quad (2.20)$$

To show that the second term of (2.15) tends to zero, we deal with two cases. In the particular case that we have  $\phi^*(s) = \mathbf{x}$  and fixed  $\mathbf{x} \in \Omega$ , clearly the second term tends to zero. In the general case we can write, adding and subtracting terms appropriately,

$$\begin{aligned} \int_t^1 \mathbf{v}^n(\phi^*(s), s) - \mathbf{v}^*(\phi^*(s), s) ds &= \int_t^1 \mathbf{v}^n(\phi^*(s), s) - \mathbf{v}^n(\phi^m(s), s) ds \\ &+ \int_t^1 \mathbf{v}^n(\phi^m(s), s) - \mathbf{v}^*(\phi^m(s), s) ds + \int_t^1 \mathbf{v}^*(\phi^m(s), s) - \mathbf{v}^*(\phi^*(s), s) ds. \end{aligned} \quad (2.21)$$

We can use similar arguments to those used in (2.16), to write

$$\begin{aligned} \left\| \int_t^1 \mathbf{v}^n(\phi^*(s), s) - \mathbf{v}^n(\phi^m(s), s) ds \right\|_{\mathbb{R}^d} &\leq \int_t^1 \|\mathbf{v}^n(\phi^*(s), s) - \mathbf{v}^n(\phi^m(s), s)\|_{\mathbb{R}^d} ds \\ &\leq C \int_t^1 \|\phi^*(s) - \phi^m(s)\|_{\mathbb{R}^d}^\alpha ds, \end{aligned} \quad (2.22)$$

where  $\alpha$  and  $C$  are the constants from Hölder continuity. Hence the first term of (2.21) tends to zero as  $n \rightarrow \infty$ . Similarly the third term of (2.21) tends to zero as  $n \rightarrow \infty$ .

Examining the second term of (2.21), we introduce a sequence of piecewise constant approximations  $\phi^m$  to  $\phi^*$  such that

$$\phi^*(s) = \lim_{m \rightarrow \infty} \phi^m(s), \quad \forall s \in [t, 1].$$

Let the elements of the sequence be constructed in the following way,

$$\phi^m(s) = \begin{cases} a_1, & s \in (t, t + \epsilon_1) \\ a_2, & s \in (t + \epsilon_1, t + \epsilon_1 + \epsilon_2) \\ \vdots & \vdots \\ a_q, & s \in (t + \sum_{i=1}^{q-1} \epsilon_i, 1), \end{cases}$$

where the function takes  $q$  constant, not necessarily distinct, values  $a_1, \dots, a_q \in \Omega$  over intervals of length  $\epsilon_1, \dots, \epsilon_q$ . So we have for the second term of (2.21)

$$\begin{aligned} \int_t^1 (\mathbf{v}^n(\phi^m(s), s) - \mathbf{v}^*(\phi^m(s), s)) ds &= \\ &\int_t^{t+\epsilon_1} (\mathbf{v}^n(a_1, s) - \mathbf{v}^*(a_1, s)) ds + \dots + \int_{t+\sum_{i=1}^{q-1} \epsilon_i}^1 (\mathbf{v}^n(a_q, s) - \mathbf{v}^*(a_q, s)) ds. \end{aligned}$$

So by (2.20), we see that the second term of (2.21) tends to zero as  $n \rightarrow \infty$ , since all arguments to  $\mathbf{v}^*$  and  $\mathbf{v}^n$  are constant. Hence we conclude for all  $t \in [0, 1]$ ,

$$\int_t^1 (\mathbf{v}^n(\phi^*(s), s) - \mathbf{v}^*(\phi^*(s), s)) ds \rightarrow 0 \quad \text{as } n \rightarrow \infty$$

and therefore we have

$$\begin{aligned}\phi^*(t) &= \lim_{n \rightarrow \infty} \phi^n(t) = \lim_{n \rightarrow \infty} \int_t^1 \mathbf{v}^n(\phi^n(s), s) ds + \mathbf{x} \\ &= \int_t^1 \mathbf{v}^*(\phi^*(s), s) ds + \mathbf{x}.\end{aligned}$$

Differentiating with respect to  $t$ ,

$$\mathbf{v}^*(\phi^*(t), t) = \frac{d\phi^*(t)}{dt},$$

which shows that  $\phi^*(t)$  conforms to the required constraint, since letting  $\phi^*(t) = \mathbf{x}_i^*(t)$  gives

$$\frac{d\mathbf{x}_i^*(t)}{dt} = \mathbf{v}^*(\mathbf{x}_i^*(t), t).$$

Since  $\phi^n$  is a convergent subsequence of  $\mathbf{x}^n$ , and  $\sup_{0 \leq t \leq 1} |\phi^n(t) - \phi^*(t)| \rightarrow 0$  as  $n \rightarrow \infty$ , we have  $\phi^n(0) = \mathbf{P}_i$ ,  $\phi^n(1) = \mathbf{Q}_i$ .

Hence we see that there exist deformation fields and control point paths in the feasible set that minimise  $\|\mathbf{v}\|_V^2$ .  $\square$

### 3 Representation as a finite linear combination of Green's functions

We define the representative of a functional and show that the velocity field can be expanded as a finite linear combination of Green's functions with zero Dirichlet boundary conditions without introducing any approximation. In particular, for a given set of control paths  $\mathbf{x}_i$ , we have an explicit expression for the deformation field  $\mathbf{v}$ .

**Theorem 2** *Riesz Representation Theorem* - To each bounded linear functional,  $\Phi$  on a Hilbert space  $\mathcal{H}$ , there corresponds an element  $u \in \mathcal{H}$  such that

$$\Phi(f) = \langle f, u \rangle_{\mathcal{H}} \quad \forall f \in \mathcal{H}.$$

The element  $u$  is called the representative of  $\Phi$  in  $\mathcal{H}$ .

**Theorem 3** *Cheney and Light* (see [5] for proof) - Let  $\Phi_1, \dots, \Phi_{n_c}$  be continuous linear functionals on a Hilbert space,  $\mathcal{H}$ . Suppose we have, for some unknown element,  $\mathbf{f}$ , a set of numerical values  $\Phi_1(\mathbf{f}), \dots, \Phi_{n_c}(\mathbf{f})$ . Then  $\mathbf{f}$  can be any element in the manifold  $M = \{\mathbf{m} \in \mathcal{H} : \Phi_i(\mathbf{m}) = \Phi_i(\mathbf{f}), 1 \leq i \leq n_c\}$ . Suppose  $\mathbf{v}_{min}$  is the element of  $M$  with minimal norm, known as the minimal norm interpolant. Then for

$$Y = \{\mathbf{y} \in \mathcal{H} : \Phi_i(\mathbf{y}) = 0, 1 \leq i \leq n_c\},$$

we have  $\mathbf{v}_{min} \perp Y$ .

We adapt a theorem taken from Cheney and Light [5] to show that the velocity fields can be expanded in terms of their representatives.

**Theorem 4** Let  $\Phi_1, \dots, \Phi_{n_c}$  be continuous linear functionals on a Hilbert space,  $\mathcal{H}$ , with representatives  $u_1, \dots, u_{n_c} \in \mathcal{H}$  respectively. Suppose for some unknown element  $h \in \mathcal{H}$ ,

we have values  $\Phi_1(h), \dots, \Phi_{n_c}(h)$ . Then  $h$  is some element of the manifold  $M = \{m \in \mathcal{H} : \Phi_i(m) = \Phi_i(h), 1 \leq i \leq n_c\}$ . Suppose  $h_{\min}$  is the element with minimal norm, the minimal norm interpolant. Then  $h_{\min} = \sum_{j=1}^{n_c} \alpha_j u_j$ , where the coefficients  $\alpha_j$  solve the system of linear equations

$$\sum_{j=1}^{n_c} \alpha_j \langle u_i, u_j \rangle = \langle h, u_i \rangle. \quad (3.1)$$

**Proof** Let

$$\begin{aligned} Y &= \{\mathbf{y} \in \mathcal{H} : \Phi_i(\mathbf{y}) = 0, 1 \leq i \leq n_c\} \\ &= \{\mathbf{y} \in \mathcal{H} : \langle \mathbf{y}, u_i \rangle = 0, 1 \leq i \leq n_c\} \\ &= \bigcap_{i=1}^{n_c} u_i^\perp. \end{aligned}$$

Now,  $h_{\min}$  is characterised by the properties  $h_{\min} \perp Y$  (from Theorem 3) and  $\Phi_i(h_{\min}) = \Phi_i(h)$  for  $1 \leq i \leq n_c$ . Since  $h_{\min} \in (\bigcap_{i=1}^{n_c} u_i^\perp)^\perp$ , we can infer that  $h_{\min} \in \text{span}\{u_1, \dots, u_{n_c}\}$ . Writing  $h_{\min} = \sum_{j=1}^{n_c} \alpha_j u_j$ , we have

$$\Phi_i(h) = \Phi_i(h_{\min}) = \sum_{j=1}^{n_c} \alpha_j \Phi_i(u_j) \quad (1 \leq i \leq n_c).$$

Thus the coefficients  $\alpha_j$  solve the system of linear equations (3.1) described.  $\square$

In Theorem 1, we have shown that a solution to the minimization problem  $\min_{\mathbf{x}, \mathbf{v}} \|\mathbf{v}\|_V^2$  exists. Now we show that the velocity field in the solution can be represented as a finite linear combination of Green's functions.

**Theorem 5** *Let  $d = 2$ . The solution  $\mathbf{v}$  to the problem of Theorem 1 can be written in the form*

$$\mathbf{v}(\mathbf{x}, t) = \sum_{i=1}^{n_c} \alpha_i(t) G(\mathbf{x}_i(t), \mathbf{x}),$$

where  $G(\cdot, \cdot)$  is a Green's function with zero Dirichlet boundary conditions with coefficients  $\alpha_i(t) \in \mathbb{R}^d$ .

**Proof** We apply Theorem 4 in our case. We define a set of continuous linear functionals on  $H$  for fixed  $k \in 1, \dots, d$  so that we examine one row of the representation, for fixed time,  $t$  as

$$\Phi_i(h) = h(\mathbf{P}_i) \quad i = 1, \dots, n_c, \Phi_i \in H, h \in H, \quad (3.2)$$

where  $(\mathbf{P}_1, \dots, \mathbf{P}_{n_c})$  is the set of initial control point positions. We know  $\Phi_i$  to be linear and continuous and hence bounded. Therefore we know by the Riesz Representation Theorem (Theorem 2) that there exists some representative  $u_i$  of  $\Phi_i$  in  $H$  so that

$$\Phi_i(h) = \langle u_i, h \rangle_H \quad \forall h \in H, \quad (3.3)$$

where  $\langle \cdot, \cdot \rangle_H$  denotes the inner product on  $H$ .

We introduce a Green's function,  $G(\mathbf{x}, \mathbf{y})$  which behaves so that

$$\Delta^2 G(\mathbf{x}, \mathbf{y}) = \delta(\mathbf{x} - \mathbf{y}).$$

We use the biharmonic Green's function, as described in the introduction. We know this Green's function to be in  $L_2(\Omega)$  with first and second order derivatives in  $L_2(\Omega)$ . This Green's function also has zero Dirichlet boundary conditions. Hence we see that the Green's function is in  $H$ , as described in Section 2. Let  $u_i(\mathbf{x}) = G(\mathbf{x}, \mathbf{P}_i)$ . Then

$$\Delta^2 u_i(\mathbf{x}) = \delta(\mathbf{x} - \mathbf{P}_i).$$

We have

$$\begin{aligned} \langle G(\cdot, \mathbf{P}_i), h \rangle_H &= \langle \delta(\cdot - \mathbf{P}_i), h \rangle_{L_2}, \quad h \in H \\ &= \int_{\Omega} \delta(\cdot - \mathbf{P}_i) h(\cdot) d\mathbf{x} \\ &= h(\mathbf{P}_i) \quad (\text{by the sifting property of the } \delta\text{-function}). \end{aligned}$$

We have shown  $G(\cdot, \mathbf{P}_i)$  to be a representative for  $\Phi_i$  in  $H$ . Hence we see that  $G(\cdot, \mathbf{P}_k) \in H$  are representatives for  $\Phi_k$  for  $k = 1, \dots, n_n$  in  $H$ . We now apply this result for the space,  $H$ , to the space,  $V$ .

We have the minimum norm interpolant  $\mathbf{v}_{min} = (v_1(\cdot, t), \dots, v_d(\cdot, t)) \in V$ . So  $\mathbf{v}_{min}$  minimises  $\|\mathbf{v}\|_V^2$ , such that the interpolation conditions (3.4) hold. From the velocity constraint (2.3), we have interpolation conditions given by

$$\mathbf{v}(\mathbf{x}_i(t), t) = \frac{d\mathbf{x}_i(t)}{dt}, \quad (3.4)$$

when we know the paths  $\mathbf{x}_i(t)$ .

By definition of the norm on  $V$ , we have

$$\begin{aligned} \|\mathbf{v}\|_V^2 &= \int_0^1 \|\mathbf{v}(\cdot, t)\|_{H \times \dots \times H}^2 dt \\ &= \sum_{k=1}^d \int_0^1 \|v_k(\cdot, t)\|_H^2 dt. \end{aligned}$$

Examining the elements of  $\mathbf{v}$  we observe that we can separate component-wise, both in terms of time and knotpoints. Hence we see that if  $\mathbf{v}_{min}$  is a minimum on  $V$ , the element  $v_k(\cdot, t)$ ,  $k = 1, \dots, d$  minimises

$$\|v_k(\cdot, t)\|_H^2$$

such that

$$\frac{dx_{i,k}(t)}{dt} = v_k(\mathbf{x}_i(t), t),$$

where the paths  $\mathbf{x}_i(t) = (x_{i,1}(t), \dots, x_{i,d}(t))$  are known so that the left hand side of the above represents the known values as in Theorem 4.

Hence we see that  $v_k(\cdot, t)$  is in the appropriate manifold,  $M$ , for the problem, given by  $M = \{v_k(\cdot, t) \in \mathcal{H} : \frac{dx_{i,k}(t)}{dt} = v_k(\mathbf{x}_i(t), t), 1 \leq i \leq n_c\}$  and we have shown  $v_k(\cdot, t)$  to be the element of the manifold with minimal norm. Hence, by Theorem 4, we see that we

can represent the elements  $v_k$ ,  $k = 1, \dots, d$  of  $\mathbf{v}_{min}$  as

$$v_k(\cdot, t) = \sum_{i=1}^{n_c} \alpha_{i,k}(t) G(\cdot, \mathbf{x}_i),$$

where we have  $\bar{\alpha}_i(t) = (\alpha_{i,1}(t), \dots, \alpha_{i,d}(t))$ . Therefore we can represent the minimum norm interpolant of  $\mathbf{v}$  as

$$\mathbf{v}_{min}(\mathbf{x}, t) = \sum_{i=1}^{n_c} \alpha_i(t) G(\mathbf{x}_i(t), \mathbf{x}). \quad (3.5)$$

□

This expansion gives us the velocity field in a form convenient for implementation without introducing any approximation.

#### 4 Numerical Methods

We restate the Geodesic Interpolating Spline problem in a Hamiltonian dynamics framework, and solve numerically. Similar methods for computation of the solution to the problem are discussed further in [16, 14, 1].

Using the representation for the velocity field from (3.5) in (1.2)–(1.3 a), the Geodesic Interpolating Spline problem can be written as

$$\min \int_0^1 \frac{1}{2} \sum_{i,j=1}^{n_c} \alpha_i^\top \alpha_j G(\mathbf{q}_i, \mathbf{q}_j) dt \quad (4.1 a)$$

such that

$$\frac{d\mathbf{q}_i}{dt} = \sum_{j=1}^{n_c} \alpha_j G(\mathbf{q}_i, \mathbf{q}_j), \quad \mathbf{q}_i(0) = \mathbf{P}_i \quad i = 1, \dots, n_c, \quad (4.1 b)$$

where (4.1 b) gives the velocity constraint and  $\mathbf{P}_i$  is a set of knotpoints on the image to which the warp is to be applied.

We can treat this as a Lagrangian by setting

$$L(\mathbf{q}, \dot{\mathbf{q}}) = \frac{1}{2} \sum_{i,j=1}^{n_c} \alpha_i^\top \alpha_j G(\mathbf{q}_i, \mathbf{q}_j), \quad (4.2)$$

where  $\mathbf{q} = (\mathbf{q}_1, \dots, \mathbf{q}_{n_c})$  and  $\dot{\mathbf{q}} = (\dot{\mathbf{q}}_1, \dots, \dot{\mathbf{q}}_{n_c}) = (\frac{d\mathbf{q}_1}{dt}, \dots, \frac{d\mathbf{q}_{n_c}}{dt})$  represent position and velocity respectively. We see that the Hamiltonian of the system is the Legendre transform of the Lagrangian function as a function of the velocity  $\dot{\mathbf{q}}$ . The generalised momentum is given by

$$\frac{\partial L}{\partial \dot{\mathbf{q}}} = \mathcal{G}^{-1} \mathcal{G} \alpha = \alpha. \quad (4.3)$$

Hence, we have the coupled system of Hamiltonian equations

$$\dot{\mathbf{q}} = \frac{\partial H}{\partial \alpha}, \quad (4.4 a)$$

$$\dot{\boldsymbol{\alpha}} = -\frac{\partial H}{\partial \mathbf{q}}, \quad (4.4 b)$$

with initial conditions

$$\begin{bmatrix} \mathbf{q}(0) \\ \boldsymbol{\alpha}(0) \end{bmatrix} = \begin{bmatrix} \mathbf{P} \\ \mathbf{A} \end{bmatrix} = \mathbf{Y}, \quad (4.5)$$

where  $\mathbf{P}$  is the vector of initial knotpoint positions in (4.1 b) and  $\mathbf{A}$  is the initial vector of generalised momentum.

The system (4.1 a)–(4.1 b) is equivalent to the nonlinear system of equations  $\Phi(\mathbf{A}; \mathbf{P}) = \mathbf{Q}$  which we solve for  $\mathbf{A}$  as a shooting problem, where  $\Phi(\mathbf{A}; \mathbf{P}) := \mathbf{q}(1)$ , the position component of the solution of the Hamiltonian system

$$\frac{d}{dt} \mathbf{q}_i = \sum_{j=1}^{n_c} \alpha_j G(\mathbf{q}_i, \mathbf{q}_j), \quad (4.6)$$

$$\frac{d}{dt} \alpha_i = -\sum_{j=1}^{n_c} \alpha_i^\top \alpha_j \frac{\partial}{\partial \mathbf{q}_j} G(\mathbf{q}_i, \mathbf{q}_j), \quad i = 1, \dots, n_c, \quad (4.7)$$

with initial conditions given in (4.5).

To solve (4.6) and (4.7), we discretise in time. We choose to discretise using the Forward Euler method. Experiments with symplectic methods have shown no advantage for this problem, principally because it is a boundary value problem where long time simulations are not of interest, and no suitable explicit symplectic integrators are available [12, 13]. Using the notation  $\mathbf{q}_i^n \approx \mathbf{q}_i(n\Delta t)$ ,  $\alpha_i^n \approx \alpha_i(n\Delta t)$ ,  $n = 0, \dots, N$ ,  $\Delta t = 1/N$ , we have

$$\begin{bmatrix} \mathbf{q}^{n+1} \\ \boldsymbol{\alpha}^{n+1} \end{bmatrix} = \begin{bmatrix} \mathbf{q}^n \\ \boldsymbol{\alpha}^n \end{bmatrix} + \Delta t \begin{bmatrix} \frac{H(\mathbf{q}^n, \boldsymbol{\alpha}^n)}{\partial \mathbf{q}} \\ -\frac{H(\mathbf{q}^n, \boldsymbol{\alpha}^n)}{\partial \boldsymbol{\alpha}} \end{bmatrix}, \quad \begin{bmatrix} \mathbf{P} \\ \mathbf{A} \end{bmatrix} = \begin{bmatrix} \mathbf{q}^0 \\ \boldsymbol{\alpha}^0 \end{bmatrix} = \mathbf{Y}. \quad (4.8)$$

We wish to examine the variation with respect to the initial momentum,  $\mathbf{A}$  in order to provide Jacobians for the nonlinear solver. The initial positions,  $\mathbf{P}$  remain fixed. Using the Forward Euler scheme for some function  $\mathbf{f}$ , we have  $\mathbf{X}^{n+1} = \mathbf{X}^n + \Delta t \mathbf{f}(\mathbf{X}^n)$  with initial condition  $\mathbf{X}^0 = \mathbf{Y}$ . Differentiating with respect to  $\mathbf{A}$  gives

$$\frac{d\mathbf{X}^{n+1}}{d\mathbf{A}} = \frac{d\mathbf{X}^n}{d\mathbf{A}} + \Delta t \frac{d\mathbf{f}(\mathbf{X}^n)}{d\mathbf{X}^n} \frac{d\mathbf{X}^n}{d\mathbf{A}}, \quad \frac{d\mathbf{X}^0}{d\mathbf{A}} = [0, I]^\top, \quad (4.9)$$

where  $I$  is the  $dn_c \times dn_c$  identity matrix.

Let  $J^n$  be the Jacobian and solve numerically a coupled system of equations

$$J^{n+1} = J^n + \Delta t \frac{d\mathbf{f}(\mathbf{X}^n)}{d\mathbf{X}^n} J^n, \quad \mathbf{X}^{n+1} = \mathbf{X}^n + \Delta t \mathbf{f}(\mathbf{X}^n) \quad (4.10)$$

with initial conditions  $J^0 = [0, I]^\top$ ,  $\mathbf{X}^0 = \mathbf{Y}$ . In our problem, we have

$$\mathbf{f}(\mathbf{X}) = \begin{bmatrix} \frac{\partial H}{\partial \mathbf{q}} \\ -\frac{\partial H}{\partial \boldsymbol{\alpha}} \end{bmatrix}, \quad \mathbf{X} = \begin{bmatrix} \mathbf{q} \\ \boldsymbol{\alpha} \end{bmatrix}, \quad \frac{d\mathbf{f}(\mathbf{X}^n)}{d\mathbf{X}^n} = \begin{bmatrix} \frac{\partial^2 H}{\partial \mathbf{q} \partial \boldsymbol{\alpha}} & \frac{\partial^2 H}{\partial \boldsymbol{\alpha}^2} \\ -\frac{\partial^2 H}{\partial \mathbf{q}^2} & -\frac{\partial^2 H}{\partial \boldsymbol{\alpha} \partial \mathbf{q}} \end{bmatrix}. \quad (4.11)$$

The entries of the Jacobian in (4.11) can be calculated explicitly. The analytic calculation of the Jacobian permits efficient solution of the nonlinear equation  $\Phi(\mathbf{A}; \mathbf{P}) = \mathbf{Q}$  using

the nonlinear iterative solver `nag_nlin_sys_sol` developed by the Numerical Algorithms Group (NAG) [19]. The solver is based on MINPACK routines, described in [18].

We calculate the entries of (4.11). We have

$$\begin{aligned} H(\boldsymbol{\alpha}, \mathbf{q}) &= \frac{1}{2} \sum_{i,j=1}^{n_c} \boldsymbol{\alpha}_i^\top \boldsymbol{\alpha}_j G(\mathbf{q}_i, \mathbf{q}_j) \\ &= \sum_{i < j} \boldsymbol{\alpha}_i^\top \boldsymbol{\alpha}_j G(\mathbf{q}_i, \mathbf{q}_j) + \frac{1}{2} \sum_{i=1}^{n_c} \boldsymbol{\alpha}_i^\top \boldsymbol{\alpha}_i G(\mathbf{q}_i, \mathbf{q}_i), \end{aligned}$$

where we use the notation  $\sum_{i < j}$  to denote summation from 1 to  $n_c$  such that  $i < j$ . We obtain first order derivatives

$$\frac{\partial H}{\partial \boldsymbol{\alpha}_k} = \sum_{j=1}^{n_c} \boldsymbol{\alpha}_j G(\mathbf{q}_k, \mathbf{q}_j), \quad (4.12)$$

$$\frac{\partial H}{\partial \mathbf{q}_k} = \sum_{i \neq k} \boldsymbol{\alpha}_i^\top \boldsymbol{\alpha}_k \frac{\partial G(\mathbf{q}_i, \mathbf{q}_k)}{\partial \mathbf{q}_k} + \frac{1}{2} \boldsymbol{\alpha}_k^\top \boldsymbol{\alpha}_k \frac{\partial G(\mathbf{q}_k, \mathbf{q}_k)}{\partial \mathbf{q}_k}. \quad (4.13)$$

Then we can calculate second derivatives

$$\frac{\partial^2 H}{\partial \boldsymbol{\alpha}_k \partial \boldsymbol{\alpha}_l} = G(\mathbf{q}_k, \mathbf{q}_l) I, \quad (4.14)$$

$$\frac{\partial^2 H}{\partial \boldsymbol{\alpha}_k \partial \mathbf{q}_l} = \boldsymbol{\alpha}_l \frac{\partial G(\mathbf{q}_k, \mathbf{q}_l)}{\partial \mathbf{q}_l}, \quad (4.15)$$

$$\frac{\partial^2 H}{\partial \boldsymbol{\alpha}_k \partial \mathbf{q}_k} = \sum_{j=1}^{n_c} \boldsymbol{\alpha}_j \frac{\partial G(\mathbf{q}_k, \mathbf{q}_j)}{\partial \mathbf{q}_k}, \quad (4.16)$$

$$\frac{\partial^2 H}{\partial \mathbf{q}_k \partial \mathbf{q}_l} = \boldsymbol{\alpha}_k^\top \boldsymbol{\alpha}_l \frac{\partial^2 G(\mathbf{q}_k, \mathbf{q}_l)}{\partial \mathbf{q}_k \partial \mathbf{q}_l}, \quad (4.17)$$

$$\frac{\partial^2 H}{\partial \mathbf{q}_k \partial \mathbf{q}_k} = \boldsymbol{\alpha}_k^\top \boldsymbol{\alpha}_k \frac{\partial^2 G(\mathbf{q}_k, \mathbf{q}_k)}{\partial \mathbf{q}_k \partial \mathbf{q}_k}, \quad (4.18)$$

(where  $I$  is the  $d$ -dimensional identity matrix). Then we can step forward using the Forward Euler scheme (4.10) to find control point paths for the system. Using this method, a 123 point test set was solved in less than 40 seconds using a single processor desktop computer.

## 5 The Diffeomorphic property under numerical approximation

The deformation field,  $\mathbf{v}$ , defines a mapping,  $\Phi$ , which we show to be diffeomorphic in the case  $d = 2$  under numerical approximation. Before proceeding, we show an important inequality.

**Proposition 2** *Let  $d = 2$ . The minimizing deformation field  $\mathbf{v} \in V$  is Lipschitz continuous so that for some  $K > 0$ , we have*

$$\|\mathbf{v}(\mathbf{x}, t) - \mathbf{v}(\mathbf{y}, t)\|_{\mathbb{R}^d} \leq K \|\mathbf{x} - \mathbf{y}\|_{\mathbb{R}^d}, \quad 0 \leq t \leq 1, \quad \mathbf{x}, \mathbf{y} \in \Omega.$$

**Proof** We have a representation for  $\mathbf{v}$  (3.5) from Theorem 5 in terms of  $\boldsymbol{\alpha}_i(t), \mathbf{x}_i(t), i = 1, \dots, n_c$ . The Green's function is globally Lipschitz continuous for  $d = 2$ , and the coefficients are continuous on a compact domain and so bounded. Hence we see that  $\mathbf{v}$  is Lipschitz continuous.  $\square$

We examine the differential equation

$$\frac{d\mathbf{x}_i(t)}{dt} = \mathbf{v}(\mathbf{x}_i(t), t), \quad \mathbf{x}_i(0) = \mathbf{P}_i, \quad \mathbf{x}_i(t) \in \Omega, \quad (5.1)$$

with  $\mathbf{v} \in V$ . Define a mapping  $\Phi : \Omega \rightarrow \Omega$  such that  $\Phi(\mathbf{P}_i) = \mathbf{x}_i(1)$ ,  $i = 1, \dots, n_c$ . By standard arguments (see, for instance [21]) and using the  $\mathbf{v}$  is Lipschitz, we see that  $\Phi$  defines a diffeomorphism on the domain,  $\Omega$ .

We discretise the mapping for the purposes of computation. We need to be certain that the mapping will retain its diffeomorphic quality under this discretization.

We define a discretised mapping which we show to be well defined, by the Contraction Mapping Theorem, and to be continuous with a well defined, continuous inverse and hence show the discretised mapping to be a homeomorphism on a unit ball,  $\Omega$  in the case  $d = 2$ . We can then see by the Inverse Mapping Theorem that the discretised mapping is diffeomorphic.

We examine the mapping,  $\Phi_{\Delta t}$ , where  $\Phi_{\Delta t}$  is a time one mapping calculated using a Forward Euler numerical scheme with  $N$  time steps of size  $\Delta t$ , where  $N\Delta t = 1$ . We use the notation  $\Phi_{\Delta t}^n(X)$  to denote  $X^n$ , the value of the  $n^{\text{th}}$  time step mapping. Then we have

$$\Phi_{\Delta t}^{n+1}(\mathbf{P}_i) = \Phi_{\Delta t}^n(\mathbf{P}_i) + \Delta t \mathbf{v}(\Phi_{\Delta t}^n(\mathbf{P}_i), n\Delta t), \quad i = 1, \dots, n_c, \quad \mathbf{P}_i \in \Omega. \quad (5.2)$$

**Theorem 6** *Let  $d = 2$ . The mapping,  $\Phi_{\Delta t} : \Omega \rightarrow \Omega$  is a diffeomorphism for  $\Delta t < \frac{1}{K}$ , where  $K$  is the Lipschitz constant of the deformation field  $\mathbf{v}$ , recalling that  $\mathbf{v}$  is Lipschitz continuous by Proposition 2 and has zero Dirichlet boundary conditions on  $\partial\Omega$  where  $\Omega$  is the unit ball.*

**Proof** We consider two cases, as shown in Figure 1. First, we show that  $\Phi_{\Delta t}$  maps from  $\Omega$  into  $\Omega$ .

In the first case, suppose  $\mathbf{P}_i \in \partial\Omega$ . Then  $\Phi_{\Delta t}^{n+1}(\mathbf{P}_i) = \Phi_{\Delta t}^n(\mathbf{P}_i)$  due to the boundary conditions, and so clearly we have  $\Phi_{\Delta t}^{n+1}(\mathbf{P}_i) \in \Omega$ .

Now we examine the more general case,  $\Phi_{\Delta t}^n(\mathbf{P}_i) \in \Omega$ . Applying the triangle inequality for norms to (5.2), we can write

$$\|\Phi_{\Delta t}^{n+1}(\mathbf{P}_i)\|_{\mathbb{R}^d} \leq \|\Phi_{\Delta t}^n(\mathbf{P}_i)\|_{\mathbb{R}^d} + \Delta t \|\mathbf{v}(\Phi_{\Delta t}^n(\mathbf{P}_i), n\Delta t)\|_{\mathbb{R}^d}.$$

The Lipschitz continuity of  $\mathbf{v}$  gives

$$\|\mathbf{v}(\Phi_1, s) - \mathbf{v}(\Phi_2, s)\|_{\mathbb{R}^d} \leq K \|\Phi_1 - \Phi_2\|_{\mathbb{R}^d}, \quad K < \infty, \quad \Phi_1, \Phi_2 \in \Omega, \quad 0 \leq s \leq 1,$$

and so we can write

$$\left\| \mathbf{v} \left( \frac{\Phi_{\Delta t}^n(\mathbf{P}_i)}{\|\Phi_{\Delta t}^n(\mathbf{P}_i)\|_{\mathbb{R}^d}}, s \right) - \mathbf{v}(\Phi_{\Delta t}^n(\mathbf{P}_i), s) \right\|_{\mathbb{R}^d} \leq K \left\| \frac{\Phi_{\Delta t}^n(\mathbf{P}_i)}{\|\Phi_{\Delta t}^n(\mathbf{P}_i)\|_{\mathbb{R}^d}} - \Phi_{\Delta t}^n(\mathbf{P}_i) \right\|_{\mathbb{R}^d}.$$



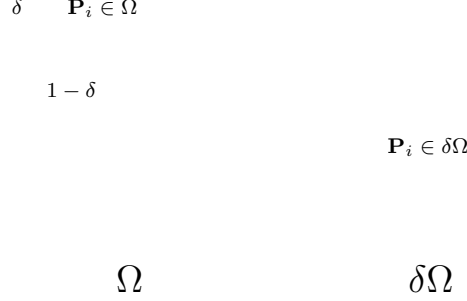


FIGURE 1. Visualization of the Proof of Theorem 6

Since we know  $\frac{\Phi_{\Delta t}^n(\mathbf{P}_i)}{\|\Phi_{\Delta t}^n(\mathbf{P}_i)\|_{\mathbb{R}^d}} \in \partial\Omega$ , we have  $\mathbf{v}\left(\frac{\Phi_{\Delta t}^n(\mathbf{P}_i)}{\|\Phi_{\Delta t}^n(\mathbf{P}_i)\|_{\mathbb{R}^d}}, s\right) = 0$ , so we have

$$\|\mathbf{v}(\Phi_{\Delta t}^n(\mathbf{P}_i), s)\|_{\mathbb{R}^d} \leq K \left\| \frac{\Phi_{\Delta t}^n(\mathbf{P}_i)}{\|\Phi_{\Delta t}^n(\mathbf{P}_i)\|_{\mathbb{R}^d}} - \Phi_{\Delta t}^n(\mathbf{P}_i) \right\|_{\mathbb{R}^d}.$$

Hence we have

$$\|\Phi_{\Delta t}^{n+1}(\mathbf{P}_i)\|_{\mathbb{R}^d} \leq \|\Phi_{\Delta t}^n(\mathbf{P}_i)\|_{\mathbb{R}^d} + K\Delta t \left\| \frac{\Phi_{\Delta t}^n(\mathbf{P}_i)}{\|\Phi_{\Delta t}^n(\mathbf{P}_i)\|_{\mathbb{R}^d}} - \Phi_{\Delta t}^n(\mathbf{P}_i) \right\|_{\mathbb{R}^d}.$$

Now, without loss of generality, suppose  $\|\Phi_{\Delta t}^n(\mathbf{P}_i)\|_{\mathbb{R}^d} = 1 - \delta$ ,  $\delta > 0$ .

We have  $\left\| \frac{\Phi_{\Delta t}^n(\mathbf{P}_i)}{\|\Phi_{\Delta t}^n(\mathbf{P}_i)\|_{\mathbb{R}^d}} \right\|_{\mathbb{R}^d} = 1$ , so we can write

$$\begin{aligned} \|\Phi_{\Delta t}^{n+1}(\mathbf{P}_i)\|_{\mathbb{R}^d} &\leq 1 - \delta + K\Delta t(1 - (1 - \delta)) \\ &\leq 1 - \delta + K\Delta t\delta. \end{aligned}$$

Since  $\Phi_{\Delta t}^{n+1}(\mathbf{P}_i) \in \Omega$  for  $\|\Phi_{\Delta t}^{n+1}(\mathbf{P}_i)\|_{\mathbb{R}^d} \leq 1$ , we see that  $\Phi_{\Delta t}^{n+1}(\mathbf{P}_i) \in \Omega$  for

$$\begin{aligned} 1 - \delta + K\Delta t\delta &\leq 1 \\ K\Delta t\delta &\leq \delta \\ K\Delta t &\leq 1. \end{aligned}$$

Hence we conclude  $\Phi_{\Delta t} : \Omega \rightarrow \Omega$  for  $\Delta t \leq \frac{1}{K}$ , meaning that the behaviour of the required  $\Delta t$  is independent of the position of the points, and only depends on the Lipschitz constant of the function,  $\mathbf{v}$ .

We see that  $\Phi_{\Delta t}$  has a unique solution by the same argument as that for the non-discretised case. Now we show  $\Phi_{\Delta t}$  to be continuous. We adapt a proof from Stuart and Humphries [21].

Suppose we have points  $\mathbf{P}_1, \mathbf{P}_2 \in \Omega$ . Then, at the first time step, we have  $\Phi_{\Delta t}^1(\mathbf{P}_1) = \mathbf{P}_1 + \mathbf{v}(\mathbf{P}_1, 0)$ ,  $\Phi_{\Delta t}^1(\mathbf{P}_2) = \mathbf{P}_2 + \mathbf{v}(\mathbf{P}_2, 0)$ , and so

$$\begin{aligned} \|\Phi_{\Delta t}^1(\mathbf{P}_1) - \Phi_{\Delta t}^1(\mathbf{P}_2)\|_{\mathbb{R}^d} &\leq \|\mathbf{P}_1 - \mathbf{P}_2\|_{\mathbb{R}^d} + \Delta t \|\mathbf{v}(\mathbf{P}_1, 0) - \mathbf{v}(\mathbf{P}_2, 0)\|_{\mathbb{R}^d} \\ &\leq \|\mathbf{P}_1 - \mathbf{P}_2\|_{\mathbb{R}^d} + K\Delta t \|\mathbf{P}_1 - \mathbf{P}_2\|_{\mathbb{R}^d} \\ &\leq (K\Delta t + 1) \|\mathbf{P}_1 - \mathbf{P}_2\|_{\mathbb{R}^d} \end{aligned} \quad (5.3)$$

where  $K$  is the Lipschitz constant for  $\mathbf{v}$ . Hence  $\Phi_{\Delta t}$  is continuous for the first time step and similarly will be continuous over all  $N$  time steps.

We define an inverse mapping  $\Psi_{\Delta t}^n$  such that  $\Psi_{\Delta t}^0(\mathbf{Q}_i) = \mathbf{Q}_i$  and such that  $\Psi_{\Delta t}^N(\mathbf{Q}_i) = \mathbf{P}_i$ ,  $i = 1, \dots, n_c$ . This inverse mapping is generated by the Backward Euler scheme

$$\Psi_{\Delta t}^{n+1}(\mathbf{Q}_i) = \Psi_{\Delta t}^n(\mathbf{Q}_i) - \Delta t \mathbf{v}(\Psi_{\Delta t}^{n+1}(\mathbf{Q}_i), (n+1)\Delta t).$$

First, we show that this mapping is well defined.

We can define a mapping,  $\mathcal{M}$ , as

$$\mathcal{M}(\Psi) = \mathbf{Q}_i + \Delta t \mathbf{v}(\Psi, n\Delta t).$$

In order to use the Contraction Mapping Theorem, we show  $\mathcal{M}$  to be a contraction. Suppose we have two points  $\Psi_1, \Psi_2 \in \Omega$ . Then we can write

$$\begin{aligned} \|\mathcal{M}(\Psi_1) - \mathcal{M}(\Psi_2)\|_{\mathbb{R}^d} &= \|\mathbf{Q}_i - \mathbf{Q}_i + \Delta t(\mathbf{v}(\Psi_1, s) - \mathbf{v}(\Psi_2, s))\|_{\mathbb{R}^d}, \\ &\leq \Delta t K \|\Psi_1 - \Psi_2\|_{\mathbb{R}^d} \text{ by Lipschitz continuity of } \mathbf{v}. \end{aligned}$$

Hence we see that  $\mathcal{M}$  defines a contraction, and so  $\Psi_{\Delta t}$  is well-defined, for  $\Delta t K < 1$ . Following the approach of Stuart [21], we show that  $\Psi_{\Delta t}$  is a continuous mapping for  $\Delta t \leq \frac{1}{K}$ . Consider Backward Euler iterations

$$\Psi_{\Delta t}^{n+1}(\mathbf{Q}_i) = \Psi_{\Delta t}^n(\mathbf{Q}_i) - \Delta t \mathbf{v}(\Psi_{\Delta t}^{n+1}(\mathbf{Q}_i), (n+1)\Delta t),$$

along with a second set of iterations given by

$$\Upsilon_{\Delta t}^{n+1}(\mathbf{Q}_i) = \Upsilon_{\Delta t}^n(\mathbf{Q}_i) - \Delta t \mathbf{v}(\Upsilon_{\Delta t}^{n+1}(\mathbf{Q}_i), (n+1)\Delta t).$$

Then we have

$$\|\Psi_{\Delta t}^{n+1}(\mathbf{Q}_i) - \Upsilon_{\Delta t}^{n+1}(\mathbf{Q}_i)\|_{\mathbb{R}^d} \leq \|\Psi_{\Delta t}^n(\mathbf{Q}_i) - \Upsilon_{\Delta t}^n(\mathbf{Q}_i)\|_{\mathbb{R}^d} + \Delta t K \|\Psi_{\Delta t}^{n+1}(\mathbf{Q}_i) - \Upsilon_{\Delta t}^{n+1}(\mathbf{Q}_i)\|_{\mathbb{R}^d},$$

using the Lipschitz continuity of  $\mathbf{v}$ . Then, since  $\Delta t < \frac{1}{K}$ , we can write

$$\|\Psi_{\Delta t}^{n+1}(\mathbf{Q}_i) - \Upsilon_{\Delta t}^{n+1}(\mathbf{Q}_i)\| \leq \frac{1}{1 - K\Delta t} \|\Psi_{\Delta t}^n(\mathbf{Q}_i) - \Upsilon_{\Delta t}^n(\mathbf{Q}_i)\|. \quad (5.4)$$

So we see that the inverse mapping is continuous.

Hence we conclude that  $\Phi_{\Delta t}$  with  $\Delta t < \frac{1}{K}$  is homeomorphic on  $\Omega$ .

From (5.3) and (5.4), we see that the Jacobians of the mapping and the inverse mapping are bounded. Hence, by the Inverse Mapping Theorem, we conclude that the mapping is also diffeomorphic.  $\square$

## 6 Uniqueness of paths - proof and numerical example

We have shown that minimizing velocity fields and paths exist for the Geodesic Interpolating Spline problem, and have shown that the velocity field generated by minimizing paths is unique. It should be noted, however that the minimizing paths are not always unique, as there can be symmetric minimizing paths, which will be demonstrated by numerical experiment, and shown in Proposition 3.

**Proposition 3** *There exist combinations of start points,  $\mathbf{P}_i$ , and end points,  $\mathbf{Q}_i$ , for which there is not a unique minimiser to the problem of Theorem 1.*

**Proof** Suppose we have a set of two start points,  $\mathbf{P}_1, \mathbf{P}_2 \in \Omega$  and two corresponding end points,  $\mathbf{Q}_1, \mathbf{Q}_2 \in \Omega$  with reflective symmetry about the  $x$ -axis so that we have  $\mathbf{P}_1 = (-a, b), \mathbf{P}_2 = (-a, -b), \mathbf{Q}_1 = (a, -b), \mathbf{Q}_2 = (a, b)$ , as illustrated in Figure 2.

FIGURE 2. Illustration of Symmetric Start and End Points

Suppose, toward a contradiction, that we have unique minimizing paths  $\mathbf{x}_1, \mathbf{x}_2$  such that

$$\mathbf{x}_1(0) = \mathbf{P}_1 = R\mathbf{P}_2 = R\mathbf{x}_2(0)$$

and

$$\mathbf{x}_1(1) = \mathbf{Q}_1 = R\mathbf{Q}_2 = R\mathbf{x}_2(1),$$

where  $R$  is an operator indicating reflection about the  $x$ -axis.

The uniqueness of minimizing paths implies that we must have  $\mathbf{x}_1(t) = R\mathbf{x}_2(t)$  for all  $t \in [0, 1]$ . Consider the point where the path  $\mathbf{x}_1$  crosses the  $y$ -axis at, say  $\mathbf{x}_1(\tau) = (\alpha, 0)$ , some  $\tau \in (0, 1), \alpha \in [0, 1]$ . At this point we must have  $\mathbf{x}_2(\tau) = (\alpha, 0) = R\mathbf{x}_2(\tau)$ . Hence we have  $\mathbf{x}_1(\tau) = \mathbf{x}_2(\tau)$ . This is impossible since we have uniqueness of solution to the differential equations initialised from any point. Hence if we have  $\mathbf{x}_1(\tau) = \mathbf{x}_2(\tau)$ , we cannot have  $\mathbf{x}_1(1) = \mathbf{Q}_1$  and  $\mathbf{x}_2(1) = \mathbf{Q}_2$ , since  $\mathbf{Q}_1$  and  $\mathbf{Q}_2$  are not coincident.

Hence we conclude that there are not always unique minimizing paths for a set of start points and end points.  $\square$

There are special cases for which there are symmetric solutions of paths. To force the shooting method to find these symmetric solutions, we experiment with the choice of initial data for  $\boldsymbol{\alpha}$ .

We examine the paths for a test problem with two initial knot point positions,  $(0.2, -0.2)$  and  $(-0.2, -0.2)$  moving to final positions,  $(-0.2, 0.2)$  and  $(0.2, 0.2)$ , respectively. First, the initial  $\boldsymbol{\alpha}$  multipliers are set to 1, the default for the routine. The shooting method solver then outputs a set of final values for  $\boldsymbol{\alpha}$ , producing the paths shown on the left hand side of Figure 3. We then initialise the solver with  $-\boldsymbol{\alpha}$ . This produces the paths shown on the right hand side of Figure 3. Experiments where all elements of  $\boldsymbol{\alpha}$  and  $-\boldsymbol{\alpha}$  were initialised as either  $-1$  or  $1$ , according to the sign of the original element produced exactly the same paths as those produced by initialising with  $\boldsymbol{\alpha}$  and  $-\boldsymbol{\alpha}$ .

FIGURE 3. Symmetry Created By Changing the Initial Conditions for the Shooting Method From  $\alpha$  to  $-\alpha$

We have shown uniqueness of the velocity field generated from a given set of paths in Section 2. This experiment shows that the paths that minimise the problem are not always unique since they have symmetric equivalents for certain configurations, but from Section 2, we know that once a path has been selected from a set of symmetrically equivalent paths, there is only one possible velocity field to be generated.

## 7 Conclusion

We have extended a previous result to show that for exact landmark-matching the minimizing paths for GIS exist, with corresponding unique vector fields. We have adapted techniques from approximation theory to show that the velocity fields can be expanded as a finite linear combination of Green's functions without introducing any approximation. We introduced a numerical approximation to a formulation of the problem as a shooting problem and proved that, under sufficiently small time steps, the discrete GIS mappings are diffeomorphic, as was previously believed to be the case.

## References

- [1] S. Allasonniere, A. Trouve, and L. Younes. Geodesic shooting and diffeomorphic matching via textured meshes. In A. Rangarajan, B. C. Vemuri, and A. L. Yuille, editors, *Energy Minimization Methods in Computer Vision and Pattern Recognition, 5th International Workshop, EMMCVPR 2005, St. Augustine, FL, USA, November 9-11*, volume 3757 of *Lecture Notes in Computer Science*, pages 365–381. Springer, 2005.
- [2] T. Boggio. Sulle funzioni di green d'ordine m. *Rend. Circ. Matem. Palermo*, 20:97–135, 1905.
- [3] F.L. Bookstein. Principal warps: thin-plate splines and the decomposition of deformations. *IEEE Transactions on Pattern Analysis and Machine Intelligence*, 11(6):567–585, 1989.
- [4] V. Camion and L. Younes. Geodesic interpolating splines. In M. A. T. Figueiredo, J. Zerubia, A. K. Jain ed., volume 2134 of *Energy Minimization Methods in Computer Vision and Pattern Recognition, Lecture notes in Computer Science*, pages 513–527. Springer-Verlag, 2001.
- [5] W. Cheney and W. Light. *A Course in Approximation Theory*. Brooks/Cole, 1999.
- [6] M. P. do Carmo. *Differential geometry of curves and surfaces*. Prentice-Hall, Inc., Englewood Cliffs, New Jersey, 1976.
- [7] P. Dupuis, U. Grenander, and M. Miller. Variational problems on flows of diffeomorphism for image matching. *Quarterly of Applied Mathematics*, LVI(3):587–600, 1998.
- [8] L. Garcin and L. Younes. Geodesic matching with free extremities. *J. Math. Imaging Vision*, 25(3):329–340, 2006.
- [9] H. E. Johnson and G. E. Christensen. Consistent landmark and intensity based image registration. *IEEE Transactions on Medical Imaging*, 21(5), 2002.
- [10] S. Joshi and M. Miller. Landmark matching via large deformation diffeomorphisms. *IEEE Transactions on Image Processing*, 9(8), 2000.
- [11] S. L. Keeling and W. Ring. Medical image registration and interpolation by optical flow with maximal rigidity. *Journal of Mathematical Imaging and Vision*, 23(1):47–65, 2005.
- [12] B. Leimkuhler and S. Reich. *Simulating Hamiltonian dynamics*. Cambridge University Press, 2004.

- [13] S. Marsland and R. McLachlan. A Hamiltonian particle method for diffeomorphic image registration. Massey University Preprint, 2006.
- [14] R. I. McLachlan and S. Marsland. Discrete mechanics and optimal control for image registration. In Wayne Read and A. J. Roberts, editors, *Proceedings of the 13th Biennial Computational Techniques and Applications Conference, CTAC-2006*, volume 48 of *ANZIAM J.*, pages C1–C16, April 2007.
- [15] A. Mills. *Image Registration Based on the Geodesic Interpolating Spline*. PhD thesis, The University of Manchester, 2007.
- [16] A. Mills, T. Shardlow, and S. Marsland. Computing the geodesic interpolating spline. In *Biomedical Image Registration, Third International Workshop, WBIR 2006*, volume 4057 of *Lecture Notes in Computer Science*, pages 169–177. Springer, 2006.
- [17] J. Modersitzki. *Numerical Methods for Image Registration*. Oxford University Press, New York, 2004.
- [18] J. J. Moré, B. S. Garbow, and K. E. Hillstom. User guide for MINPACK–1. Technical Report ANL–80–74, Mathematics and Computer Sciences Division, Argonne National Laboratory, Argonne, Ill., 1980.
- [19] Numerical Algorithms Group, <http://www.nag.co.uk/numeric/FN/manual/>. *NAG Manual*.
- [20] M. Renardy and R.C. Rogers. *An Introduction to Partial Differential Equations*. Springer Verlag, 1996.
- [21] A. M. Stuart and A. R. Humphries. *Dynamical Systems and Numerical Analysis*, volume 2 of *Cambridge Monographs on Applied and Computational Mathematics*. Cambridge University Press, 1996.
- [22] A. Trouné and L. Younes. Metamorphoses through Lie group action. *Found. Comput. Math.*, 5(2):173–198, 2005.